

Contents lists available at ScienceDirect

Organic Electronics

journal homepage: www.elsevier.com/locate/orgel



Memory stabilities and mechanisms of organic bistable devices with giant memory margins based on Cu₂ZnSnS₄ nanoparticles/PMMA nanocomposites



Dong Yeol Yun, Narayanasamy Sabari Arul, Dea Uk Lee, Nam Hyun Lee, Tae Whan Kim*

Department of Electronics and Computer Engineering, Hanyang University, Seoul 133-791, Republic of Korea

ARTICLE INFO

Article history: Received 3 February 2015 Received in revised form 24 April 2015 Accepted 5 May 2015 Available online 5 May 2015

Keywords: Nonvolatile memory Giant memory margin CZTS nanoparticles/PMMA nanocomposites Switchable memory devices

ABSTRACT

Organic bistable devices (OBDs) were fabricated utilizing nanocomposites made from a blend of $\text{Cu}_2\text{ZnSnS}_4$ (CZTS) nanoparticles within a polymethyl methacrylate (PMMA) matrix on a polyethylene terephthalate substrate. Energy dispersive X-ray spectroscopy profiles, X-ray diffraction patterns, and high-resolution transmission electron microscopy images showed that the polycrystalline CZTS nanoparticles were randomly distributed in the PMMA layer. The current–voltage (I–V) curves at 300 K for the fabricated OBDs showed bidirectional switchable and current hysteresis behaviors, indicative of the removal of sneak current paths without an additional layer with characteristics of diode or selector. The removal of the sneak current paths prevented the leakage current of the OBDs, resulting in an increase of the current of high conduction (ON) level. The maximum ON/low-conduction (OFF) ratio of the current bistability for the fabricated OBDs was as large as 1×10^9 . The write–read–erase–read sequences of the OBDs showed rewritable nonvolatile memory behaviors. The ON or the OFF states could be retained for 1×10^5 cycles, indicative of excellent memory stability. The ON/OFF ratio of 10^9 was maintained after 10^5 cycles. The memory mechanisms of the fabricated OBDs are described on the basis of the I–V results.

© 2015 Elsevier B.V. All rights reserved.

1. Introduction

Organic/inorganic nanocomposites have attracted a great deal of attention due to their promising applications in diverse electronic and optoelectronic devices [1–9]. Organic bistable devices (OBDs) based on hybrid nanocomposites containing inorganic nanoparticles (NPs) have emerged as great candidates for next-generation nonvolatile memory devices because of their excellent properties of low fabrication cost, low power consumption, high data storage density, and high mechanical flexibility [10-13]. Nonvolatile memory devices with NPs added into a polymer matrix and with a subsidiary layer with a diode function have shown some significant improvements for use as bistable memory devices [14]. While the Restriction of Hazardous Substances Directive (RoHS) prohibits the utilization of compound semiconductor materials containing Cd and Pb atoms in devices, the RoHS permits the use of CZTS as these materials are environment-friendly [15].

Even though some studies concerning the formation and the physical properties of CZTS NPs have been carried out [16–20], investigations of enhancements of memory margins and achievement of memory stabilities for OBDs fabricated utilizing CZTS NPs blended into a PMMA layer on a flexible indium-tin-oxide (ITO)-coated polyethylene terephthalate (PET) substrate have not yet been reported.

This paper reports data on significant enhancements of the memory margins and achievement of memory stabilities in OBDs utilizing CZTS NPs blended into a PMMA layer. High-resolution transmission electron microscopy (HRTEM), selected area electron diffraction (SAED) pattern, energy dispersive X-ray spectroscopy (EDS), and X-ray diffraction (XRD) measurements were performed to investigate the microstructural properties of the CZTS NPs. Current-voltage (*I*–*V*) measurements were carried out to investigate the electrical current bistability and bidirectional switchability of the OBDs. The memory mechanisms of the OBDs are described on the basis of the *I*–*V* results.

E-mail address: twk@hanyang.ac.kr (T.W. Kim).

^{*} Corresponding author.

2. Experimental details

An overall schematic of the OBDs device fabrication processes is shown in Fig. 1. The detailed preparation processes and the structural properties of the CZTS NPs are described elsewhere [21]. CZTS NPs were synthesized by a hydrothermal method at 180 °C for 6 h using Cu, Zn, Sn chloride precursors along with thiourea as a precipitating agent. The obtained precipitate was centrifuged, washed, and dried in vacuum oven at 80 °C for 4 h (Fig. 1(a-c)). Subsequently, the blended solution containing 3.3-wt.% of synthesized CZTS NPs was mixed with PMMA in an N,N-dimethylformamide (DMF) solvent by using ultrasonication, as shown in Fig. 1(d). Meanwhile, the ITO-coated PET substrates were ultra-sonicated in methanol, DI water, and isopropyl alcohol for 15 min each. The cleaned substrates were blown dry by using N2 gas to evaporate the existing solvents on the substrate (Fig. 1(e)). The blended solution was dropped onto ITO-coated PET substrates and was spin-coated sequentially at 500 rpm for 5 s, 3000 rpm for 40 s, and 500 rpm for 5 s (Fig. 1(f)). After having baked the samples at 90 °C for 30 min to remove the remaining solvents and improve the uniformity of the CZTS NPs blended into the PMMA layer on the ITO-coated PET substrates. Al top electrodes with thicknesses of 140 nm and widths of 300 um were deposited on the PMMA layers containing the CZTS NPs by using thermal evaporation through a metal mask at a pressure of 1×10^{-6} Torr (Fig. 1(g)). The thickness of the PMMA layer containing the CZTS NPs, as determined using α-step equipment, was approximately 160 nm. The OBDs based on the nanocomposites are sandwiched between two Al electrodes, and the final memory device with a bidirectional selector is shown in Fig. 1(h).

EDX and HRTEM measurements (model: JEM 2100F) were done at 200 kV to investigate the chemical compositions and the morphologies of the CZTS nanoparticles. XRD patterns were measured by using a Rigaku D/MAX-2500 V diffractometer with Cu K α radiation, which was operated at a scanning rate of 5°/min over a 2θ range between 20° and 90° . The I-V and the write–read–erase–re ad characteristics were investigated by using a 4140B pA

meter/DC voltage source and an Agilent 3250A 80-MHz function/arbitrary waveform generator, respectively.

3. Results and discussion

Fig. 2 shows plane-view TEM images, a SAED pattern, an EDS spectrum, and an XRD curve for synthesized CZTS NPs. The formation of the CZTS nanospheres is clearly shown in Fig. 2(a), and the inset of Fig. 2(a) depicts the SAED of the synthesized CZTS NPs. The SAED pattern shows the reflection of (112), (220), and (312) planes of the CZTS NPs, which is in reasonable agreement with XRD results. The CZTS nanospheres compose of triangle geometry CZTS NPs, indicative of the existence of the grain boundaries, as shown in Fig. 2(b), can be assigned to the kesterite phase of CZTS [21,22]. The crystallite size of the CZTS NPs in the nanospheres is approximately 4 nm, which is consistent with Scherrer equation for the X-ray diffraction pattern. The energy peaks of the EDX spectrum show that the synthesized NPs contain elemental Cu, Zn, Sn, and S, indicative of the formation of CZTS, as shown in Fig. 2(c). The atomic stoichiometries of the synthesized CZTS compositions are, on average, 26.1% Cu, 25.4% Zn, 14.1% Sn, and 34.4% S. The crystalline structure of the synthesized CZTS NPs characterized by the XRD curve is shown in Fig. 2(d). The XRD curve of the CZTS NPs exhibits three broad peaks, 28.5°, 47.6°, and 56.3°, which correspond to the diffractions from the (112), (220), and (312) planes of the CZTS NPs [21]. The HRTEM and XRD results are in reasonable agreement with those reported for polycrystalline and stoichiometric CZTS in the tetragonal phase [23]. The CZTS NPs structured by polycrystalline provide more trap sites than that of crystal for the capture of carriers [24,25].

The I-V curves at 300 K for the Al/CZTS NPs blended into PMMA layer/ITO/PET devices are shown in Fig. 3. The applied voltage across the device was varied in a sequence of 0, 4, 0, -4, and 0 V, as shown in Fig. 3(a) and (b). The I-V curves below low voltage (0 to 0.4 and 0 to -0.4 V) show bidirectional diode characteristics, indicative of the preventions of the number of sneak current paths

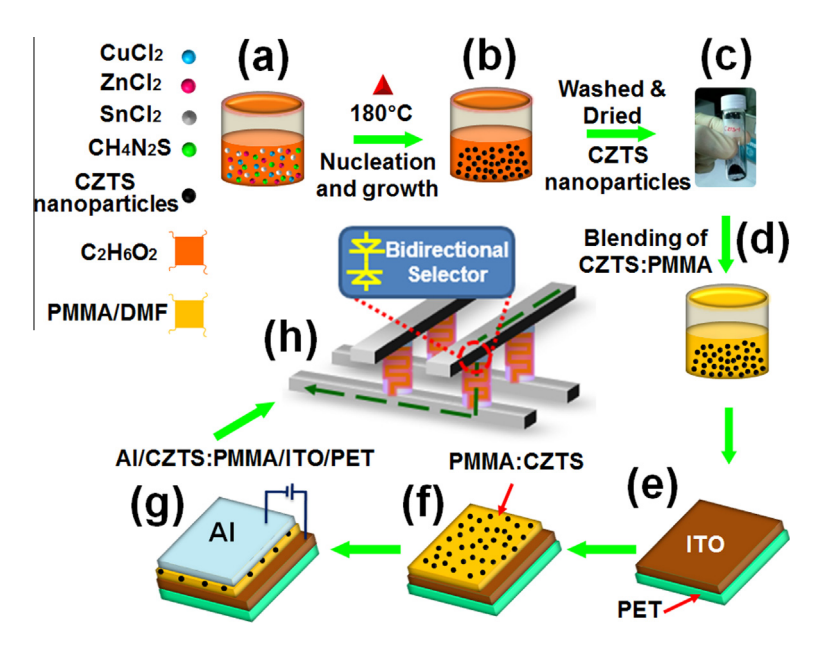


Fig. 1. Schematic diagrams of the fabrication processes for the OBDs: (a) chloride precursors of Cu, Zn, Sn, and thiourea (CH_4N_2S) were added to ethylene glycol $(C_2H_6O_2)$ and stirred well; (b) the solution was maintained at 180 °C for 6 h and then allowed to cool to room temperature, after which it was washed and dried at 60 °C to obtain the CZTS nanoparticles (NPs); (c) photographs of the CZTS NPs; (d) blending of CZTS NPs and PMMA in N,N-dimethylformamide (DMF); (e) ITO-coated PET substrates; (f) blended CZTS:PMMA layer formation on the ITO layer by using a spin-coating technique; (g) Al-electrode deposition on CZTS:PMMA/ITO/PET sheets by using a thermal evaporation process; (h) final memory device with a bidirectional selector.

Download English Version:

https://daneshyari.com/en/article/1263714

Download Persian Version:

https://daneshyari.com/article/1263714

<u>Daneshyari.com</u>